

Self- similar behavior of the Neutron Fracture Functions

Samira Shoeibi Mohsenabadi¹  * and F. Taghavi-Shahri¹  †

⁽¹⁾*Department of Physics, Ferdowsi University of Mashhad, P.O.Box 1436, Mashhad, Iran*

(Dated: December 8, 2021)

In this article, we have employed fractal formalism to calculate the Fracture Functions of the Leading neutron produced in ep collisions. The fractal concept describes the self-similar behavior of the proton structure at Leading neutron production of semi-inclusive Deep Inelastic Scattering at the low values of the fractional momentum variable β . The Fracture Functions (FFs) parameterized the non-perturbative part of the fragmentation process at the initial scale of Q_0^2 . In this analysis, we benefit from the Leading neutron (Ln) experimental data published by H1 Collaboration and in order to estimate the uncertainty of neutron FFs and corresponding observables, we used the Hessian method. As a consequence of this Next-to-Leading order QCD analysis, we achieve a nice agreement between the prediction of our model for neutron FFs and experimental data. It seems that the fractal approach based on the self-similar behavior of these conditional parton distribution functions at low x can nicely describe the experimental data.

Contents

I. Introduction	2
II. Theory setup	3
A. Fracture Functions and the Leading neutron Production	3
B. Fractals	6
C. The Validity test of using the Fractal Model In Leading neutron Production Mechanism	7
III. Essential parts of the Fractal Neutron FFs and their uncertainties	9
A. Neutron FFs in the Fractal approach	9
B. Experimental data	12
C. χ^2 minimization and nFFs Uncertainties	12

*Electronic address: Samira.Shoeibimohsenabadi@mail.um.ac.ir

†Electronic address: Taghavishahri@um.ac.ir (Corresponding author)

IV. Results and discussion	13
V. Summary and Conclusions	16
Acknowledgements	17
Appendices	19
Appendix A	19
References	21

I. INTRODUCTION

Proton is known as a strongly bound state of quarks and gluons in Quantum Chromodynamics (QCD). Considering its collisions with electron not only clarify its structure, but also reveal the dynamics of strong interaction at high energy physics [1–8]. Investigation of the Parton Distribution Functions (PDFs) and the proton structure functions at small values of x (the Bjorken scaling variable, which represents the proton momentum fraction carried by the struck quark) is interesting and the subject of some debates during the last decades [9–11]. One of the fascinating phenomenological models that well describes experimental data at low x is based on the scaling behavior or fractal behavior of PDFs [12–16]. Fractal geometry provides a new perspective to describe the natural phenomena and they are based on self-similarity symmetry with respect to scale or size: A small part of the system is approximately similar to the entire system. Benoit Mandelbrot, as a pioneer scientist, defined the fractal as a set of self-similar objects that characterized by the fractional dimension (Hausdorff dimension) which is different than the topological one [17]. The low x behavior of the proton structure is dominated by the gluon-gluon interactions which increase the gluon and the sea quark densities, leading to the self-similarity in PDFs. Recently, relevant work has been done in the investigation of the Deep Inelastic Scattering (DIS) processes [18]. The idea of considering the self-similar features in the multi partons interactions was proposed by Lastovcka [20, 21] and others have used it to investigate the proton structure functions [22–27, 30, 31]. In these references, the fractal formalism are applied to proton structure functions up to Leading Order (LO) and they do not consider the gluon densities on their analysis.

Here in this paper, we intend to use the fractal model to describe the Leading neutron production processes and calculate the neutron Fracture Functions (nFFs) in the positron-proton collisions.

These Leading neutrons are high-energy particles that carry a remarkable portion of the incoming proton energy. They are also produced at a small polar angle with respect to the positron-proton collision axis. The FFs are conditional probabilities of finding partons with flavor i and momentum fraction x while simultaneously hadron h is detected in the final states of the interaction between lepton and proton. These FFs obey evolution equations with an additional inhomogeneous term as compared to the standard Altarilli-Parisi equations [37]. They also describe the semi-inclusive DIS processes in the target fragmentation region [32–40]. Although they play a fundamental role in describing the semi-inclusive DIS processes and the global analysis requires their shapes at a given initial scale, QCD is unable to provide or predict them yet. Therefore, it is not only crucial to parametrize them phenomenologically, but also it is necessary to use experimental data in parallel, to make a connection with perturbative QCD.

From the experimental point of view, the ZEUS and H1 collaborations published the experimental Leading baryons data [41–46]. The semi-inclusive cross-sections for the production of Leading baryons can be studied by using FFs concept [47, 59, 60].

In the following, we will investigate the cross-section of the Leading neutron production by adopting the fractal model and defining the neutron Fracture Functions, "nFFs". In Sec. II, fractals are introduced and the FFs in Leading neutron production are discussed. Furthermore, the emergence of the fractal features in Leading neutron production is examined. In Sec. III, the parametrization of the neutron FFs are provided within the fractal model and we also compared them with experimental data. The uncertainties of nFF are given, using the Hessian method. In Sec. IV, our findings are checked against H1 experimental data. In Sec. V, we finish with the summary and our conclusions.

II. THEORY SETUP

In this section, we will review the theoretical aspects of the QCD analysis performed in this paper. To begin, let us have a short review on the nFFs concept in QCD. They are also reviewed in Refs. [47, 59, 60]. We then move to the discussion of the fractal concept and its footprint in the Leading neutron production mechanism.

A. Fracture Functions and the Leading neutron Production

Inclusive DIS processes are described by three kinematic variables: $x = \frac{Q^2}{2p \cdot q}$, $Q^2 = -q^2$ and $y = \frac{p \cdot q}{p \cdot k} \simeq \frac{Q^2}{sx}$ where p , k , and q are the four-momenta of the incident proton, the incident positron and

the exchanged virtual photons, respectively. Here \sqrt{s} is the center of mass energy for positron and proton. However, semi-inclusive DIS describes the mechanism of the Leading neutrons produced in the final state by using two more kinematic variables [36]:

$$\begin{aligned} x_L &= 1 - \frac{q \cdot (p - p_n)}{q \cdot p} \simeq \frac{E_n}{E_p} \\ t &= (p - p_n)^2 \simeq -\frac{p_T^2}{x_L} - (1 - x_L) \left(\frac{m_n^2}{x_L} - m_p^2 \right) \end{aligned} \quad (1)$$

where x_L is the momentum fraction carried by the outgoing neutron and t is squared four-momentum transfer between the incoming proton and the final state neutron. In Eq. (1), m_p is the proton mass and p_n is the four-momentum of the final state neutron. The outgoing neutron energy is E_n and its transverse momentum for the incoming proton is denoted by p_T .

The four-fold differential cross-section for the Leading neutron production, $e^+p \rightarrow e^+nX$ processes, can be written as a function of semi-inclusive Leading neutron transverse and longitudinal structure functions, $F_2^{\text{Ln}(4)}$ and $F_L^{\text{Ln}(4)}$, which is defined as [37, 42, 44, 45, 49]:

$$\begin{aligned} \frac{d^4\sigma(ep \rightarrow e'nX)}{d\beta dQ^2 dx_L dt} &= \frac{4\pi\alpha^2}{\beta Q^4} \left(1 - y + \frac{y^2}{2}\right) F_2^{\text{Ln}(4)}(\beta, Q^2; x_L, t) \\ &+ F_L^{\text{Ln}(4)}(\beta, Q^2; x_L, t). \end{aligned} \quad (2)$$

The scaled fractional momentum variable β is defined by:

$$\beta = \frac{x}{1 - x_L} \quad (3)$$

In Eq. (2), $F_{2,L}^{\text{Ln}(4)}(\beta, Q^2; x_L, p_T^2)$ can also be interpreted as the sub-structure function of the proton structure functions, $F_{2,L}(x, Q^2)$ in the inclusive DIS. The t integrated differential cross section can be obtained by:

$$\begin{aligned} \frac{d^3\sigma(ep \rightarrow e'nX)}{d\beta dQ^2 dx_L} &= \int_{t_0}^{t_{min}} \frac{d^4\sigma(ep \rightarrow e'nX)}{d\beta dQ^2 dx_L dt} dt \\ &= \frac{4\pi\alpha^2}{\beta Q^4} \left(1 - y + \frac{y^2}{2}\right) F_2^{\text{Ln}(3)}(\beta, Q^2; x_L) \\ &+ F_L^{\text{Ln}(3)}(\beta, Q^2; x_L), \end{aligned} \quad (4)$$

where the integration limits are:

$$\begin{aligned} t_{min} &= -(1 - x_L) \left(\frac{m_N^2}{x_L} - m_p^2 \right), \\ t_0 &= t_{min} - \frac{(p_T^{max})^2}{x_L}. \end{aligned} \quad (5)$$

p_T^{max} is the upper limit of the neutron transverse momentum used for the $F_{2,L}^{Ln(3)}$ measurement. In this paper we define the reduced e^+p cross section $\sigma_r^{Ln(3)}$ in term of leading neutron transverse $F_2^{Ln(3)}$ and the longitudinal structure functions $F_L^{Ln(3)}$ as [42, 45]:

$$\begin{aligned} \sigma_r^{Ln(3)} &= F_2^{Ln(3)}(\beta, Q^2; x_L) \\ &- \frac{y^2}{1 + (1 - y)^2} F_L^{Ln(3)}(\beta, Q^2; x_L). \end{aligned} \quad (6)$$

By applying the factorization theorem to the semi-inclusive DIS, we can write the semi-inclusive Leading neutron transverse and longitudinal structure functions, $F_2^{Ln(4)}$ and $F_L^{Ln(4)}$, $F_2^{Ln(4)}(\beta, Q^2; x_L, p_T^2)$ as the convolution of conditional parton distribution functions, $\mathcal{M}_{i/p}^n(\beta, \mu_F^2; x_L, p_T^2)$: "**proton to neutron Fracture Functions**" and Wilson coefficient functions, C_{ki} ($k = 2, L$) [60]:

$$F_k^{Ln(4)}(\beta, Q^2; x_L, p_T^2) = \sum_i \int_\beta^1 \frac{d\xi}{\xi} \mathcal{M}_{i/p}^n(\beta, \mu_F^2; x_L, p_T^2) \times C_{ki}\left(\frac{\beta}{\xi}, \frac{Q^2}{\mu_F^2}, \alpha_s(\mu_R^2)\right) + \mathcal{O}\left(\frac{1}{Q^2}\right). \quad (7)$$

here μ_F^2 and μ_R^2 are factorization and renormalization scales, respectively and $\mathcal{M}_{i/p}^n(\beta, \mu_F^2; x_L, p_T^2)$ describes the probability of detecting Leading neutron with momentum fraction x_L and transverse momentum p_T^2 in the final state, while simultaneously the specific parton i with fraction momentum of β interacts with the virtual photon. Similar to the usual parton densities, these functions are independent of the hard scattering process and represent the objective structure of the target. They also contain rich information about the proton structure functions and non-perturbative dynamics. Integrating $F_2^{Ln(4)}(\beta, Q^2; x_L, p_T^2)$ with respect to p_T^2 , up to the small value of $p_T^{max} \ll Q^2$, enhances the relative contribution of the exchanged object. Therefore, one may interpret nFFs, $\mathcal{M}_{i/p}^n(\beta, \mu_F^2; x_L)$, as the parton distribution of the exchanged object (normally pion) between the target and the final state Leading neutron. Using limiting fragmentation hypothesis [53], $F_2^{Ln(4)}(\beta, Q^2; x_L, p_T^2)$ can be written as the pion flux factor, f , (which depends on Leading neutron variable (x_L, p_T^2)) and the pion structure function, F_2^π , (which depends on the lepton variable (β, Q^2)) [45]:

$$F_2^{Ln(4)}(\beta, Q^2; x_L, p_T^2) = f(x_L, p_T^2) F_2^\pi(\beta, Q^2) \quad (8)$$

Recently different groups [55–57] have used this equation in order to extract the pionic distribution functions by using the experimental data related to the Leading neutron production [42, 45]. It is worth mentioning that for the Leading neutron production process, the pion exchange mechanism is usually considered to be dominated at large neutron longitudinal momentum fractions x_L and nonpionic contributions become large at small x_L . The sensitivity to the one-pion exchange

contribution is considered in detail at Ref [56]. The scale dependence of the neutron FFs can be extracted from Leading neutron production processes. Integrating the proton-to-neutron FFs over p_T^2 up to the small value of $p_{T_{max}}^2 = \epsilon Q^2$ ($\epsilon < 1$), in fixed value of x_L , obey the standard DGLAP evolution equations [47, 50, 60]:

$$Q^2 \frac{\partial M_{i/p}^B(\beta, Q^2; x_L)}{\partial Q^2} = \frac{\alpha_s(Q^2)}{2\pi} \int_{\beta}^1 \frac{du}{u} P_i^j(u) M_{j/p}^B\left(\frac{\beta}{u}, Q^2; x_L\right) \quad (9)$$

where $P_i^j(u)$ are regularized Altarelli-Parisi splitting functions [51]. Although the Wilson coefficient functions are the same as those obtained in inclusive DIS and they are calculable within pQCD [52], the nFFs have non-perturbative nature and their parameterized form should be inspired by and obtained from experimental data.

B. Fractals

Fractal geometry is a new language used to describe the models and analyze the complex forms found in the nature. Plants, clouds, weather, turbulence, chaotic phenomena in fluids, biological phenomena such as biological time series or the growth pattern of bacteria and many other phenomena in nature can be modeled by the fractals. Fractals have three general properties: a) Self-similarity. b) Iterative formation. c) Fractional or fractal dimension. In mathematical language, similarity means that when the size is varied, the form would not be changed. Fig. (1) shows two samples of exact self-similar fractals. By iteration, they are made of smaller and smaller shapes. In this figure, M is the number of each side segment named as "magnification factor" and N is the number of self-similar shapes created by the segmentation. The self-similarity dimension is introduced in Ref. [17] and used to consider the proton structure function at low values of x in Refs. [20, 21]. It defines as:

$$D = \frac{\log(\text{number of self-similar objects})}{\log(\text{magnification factor})} = \frac{\log M^D}{\log M} \quad (10)$$

Using Eq. (10) for square and Sierpinski triangle fractal in Fig. (1), we achieve the dimension values of these figures as 2 and 1.5849, respectively. The fractional or fractal dimension for the Sierpinski triangle fractal indicates the degree of detail in this object and measures its complexity. The fractal dimension also demonstrates how much space it occupies between the euclidean dimensions.

Let's look at fractal dimension in more details. Eq. (10) is the definition of a fractal dimension for discrete fractals. In general, ζ is a real number and the number of self-similar objects is

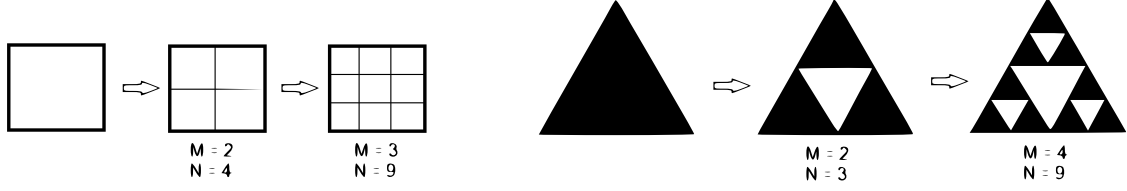


FIG. 1: (Color online) Equal segmentation of square and Sierpinski triangle fractal. M is the number of each side segment named it as magnification factor and N is the number of self-similar shapes created by the segmentation.

represented by $f(\zeta)$. Since the dimension may change with scaling, a local dimension is defined as:

$$D_f(\zeta) = \frac{\partial \log(f(\zeta))}{\partial \log(\zeta)} \quad (11)$$

For ideal mathematical fractals, mentioned above, $D_f(\zeta)$ is constant for the whole fractal ($D_f(\zeta) \equiv D$). However, there are many fractals in nature that they are not mathematically ideal and most of the time they have mono fractal structure only in a certain region of magnification. as a result, introducing a scale dependent dimension is not weird. If we consider a region on which the the dimension is approximately constant, we can rewrite the Eq.(11) as:

$$D = \frac{\partial \log f(\zeta)}{\partial \log \zeta} \quad (12)$$

Therefore, the density function can be written as:

$$\log f(\zeta) = D \cdot \log \zeta + D_0 \quad (13)$$

In this relation, D_0 defines the normalization factor, and $f(\zeta)$ is a power-law function ($f(\zeta) \propto \zeta^D$) where D is the fractal dimension of this density function. The linear behavior of $\log f(\zeta)$ as $\log \zeta$ has a key role to find the magnification factor of the density function. For two independent magnification factors, ζ and η , this relation can be extended as:

$$\log f(\zeta, \eta) = D_\zeta \cdot \log \zeta + D_\eta \cdot \log \eta + D_{\zeta\eta} \cdot \log \eta \log \zeta + D_0 \quad (14)$$

$D_{\zeta\eta}$ demonstrates the dimensional correlation related to two magnification factors, ζ and η .

C. The Validity test of using the Fractal Model In Leading neutron Production Mechanism

It is known that at low x region, scale violation occurs and the parton densities rise. If we assume this region obey the fractal features, the unintegrated parton densities related to the Leading

neutron production can be described by the fractal model mentioned in section II B. In order to check whether the fractal model can be useful in describing the neutron production mechanism or not, we employ the Ref. [47] parameterization of nFFs. This enables us not only to check the validity of the model but also provides us with the magnification factor(s) of the unintegrated nFFs. The nFFs, $\mathcal{M}_{i/p}^n(\beta, Q^2; x_L)$ are defined as follows:

$$\mathcal{M}_{i/p}^n(\beta, Q^2; x_L) = \int_0^{Q^2} \mathcal{M}_{i/p}^n(\beta, k_t^2; x_L) dk_t^2 \quad (15)$$

where k_t^2 is the parton transverse momentum. Since unintegrated nFFs, $\mathcal{M}_{i/p}^n(\beta, k_t^2; x_L)$, depending on $\beta = \frac{x}{1-x_L}$, x_L and k_t^2 therefore, it seems that there are three candidates for magnification factors of unintegrated nFFs: β (or x), x_L and k_t^2 . However, according to factorization hypotheses mentioned in Refs. [48], the leading neutron transverse structure functions follow the general forms of

$$F_k^{Ln(3)}(\beta, Q^2; x_L) = f(x_L) F_k^{Ln(2)}(\beta, Q^2) \quad (16)$$

where the discrete-function $f(x_L)$ is known as chiral splitting function [56] and it describes the splitting of a proton into a πn system. In this analysis this function is expressed as five free parameters. The parametrized form for $F_2^{Ln(2)}(\beta, Q^2)$ is then based on the proton structure functions. Therefore, the two variables of β (or x) and k_t^2 are the final candidates for magnification factors of unintegrated nFFs. The behaviour of logarithmic unintegrated parton density in order of $\log(x)$ in fixed value of $Q^2 = 15 \text{ GeV}^2$, $x_L = 0.5$ and its logarithmic behaviour in order of $\log(Q^2)$ in fixed value of $x = 0.001$, $x_L = 0.5$ are shown in Fig. (2). The linear behavior is detected for $x < 0.001$ and $Q^2 > 7 \text{ GeV}^2$. If we consider the unintegrated densities as fractal, in these two regions, we can find the constant value of fractal dimension by using Eq. (12). This region known as mono fractal region, while in the other regions we expect the multi fractal behavior for those unintegrated PDFs. It means that in Eq. (11), the fractal dimension should be local one.

As mentioned in Refs. [20, 21], magnification factors have some properties, namely, they should be positive, nonzero and dimensionless. As a result, in order to satisfy the two latter features, we choose $1 + \frac{Q^2}{q_0^2}$ instead of Q^2 . In addition, when the structure is probed deeper, x goes to zero while the magnification factor should increase. Therefore, we choose $\frac{1}{x}$ instead of x . Consequently, we choose $1 + \frac{Q^2}{q_0^2}$ and $\frac{1}{x}$ as magnification factors of unintegrated parton densities in Leading neutron production mechanism.

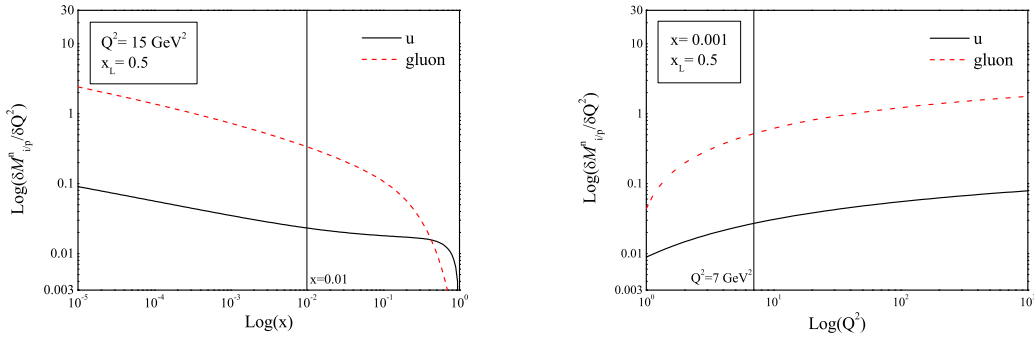


FIG. 2: (Color online) The validity test of the fractal model for Leading neutron production mechanism by using nFFs proposed in Ref [47]

III. ESSENTIAL PARTS OF THE FRACTAL NEUTRON FFs AND THEIR UNCERTAINTIES

The concept of the Fracture Functions, FFs, is useful to describe and understand the physics in the forward region. Since these universal functions cannot be calculated directly in pQCD, one needs to assume a functional form for them with a number of free parameters and then, attempt to fix the parameters by using the experimental data. Here, we introduce the parameterized form of the nFFs at an initial Q_0^2 based on the fractal model. We also briefly review the experimental data and estimation of the uncertainties.

A. Neutron FFs in the Fractal approach

Following the sections IIB and IIC and Refs. [20, 21], we introduce the unintegrated nFFs as follows:

$$\log(\mathcal{M}_{i/p}^n(\beta, k_t^2; x_L)) = \theta(x_L)[D_1^i \log(\frac{1}{\beta}) \log(1 + \frac{k_t^2}{q_0^2}) + D_2^i \log(\frac{1}{\beta}) + D_3 \log(1 + \frac{k_t^2}{q_0^2}) + D_0^i - \log(M^2)] \quad (17)$$

where q_0 is a free parameter to be determined in the analysis and $\theta(x_L)$ is a x_L -dependent function. The flavour dependent parameters in Eq. (17) are D_0^i , D_1^i and D_2^i . D_0^i fixes the normalization of $\mathcal{M}_{i/p}^n(\beta, k_t^2; x_L)$. D_1^i is the dimensional correlation relating to the β and Q^2 factors. D_2^i and D_3 are the dimensions related to the magnification factors β and Q^2 , respectively. The superscript i denotes the gluon and light quarks ($q=u, \bar{u}, d, \bar{d}, s, \text{ and } \bar{s}$). Using the parameterized form given

in Eq. (17) and Eq. (15), the initial integrated nFFs (up to Q_0^2 value) are written as:

$$\begin{aligned}\beta\mathcal{M}_{q/p}^n(\beta, Q_0^2; x_L) &= g(x_L) \cdot \frac{e^{D_0^q q_0^2 \beta^{-D_2^q+1}}}{(M^2)(1+D_3-D_1^q \log(\beta))} (\beta^{-D_1^q \log(1+\frac{Q_0^2}{q_0^2})} (1+\frac{Q_0^2}{q_0^2})^{D_3+1} - 1) \\ \beta\mathcal{M}_{g/p}^n(\beta, Q_0^2; x_L) &= g(x_L) \cdot \frac{e^{D_0^g q_0^2 \beta^{-D_2^g+1}}}{(M^2)(1+D_3-D_1^g \log(\beta))} (\beta^{-D_1^g \log(1+\frac{Q_0^2}{q_0^2})} (1+\frac{Q_0^2}{q_0^2})^{D_3+1} - 1)\end{aligned}\quad (18)$$

here $g(x_L)$ is defined as:

$$g(x_L) = N_i x_L^{A_i} (1-x_L)^{B_i} (1+C_i x_L^{D_i}) \quad (19)$$

Note that the additional term, $-\log M^2$, in Eq. (17), having dimension of energy squared, so the integrated parton distribution function defined in Eq. (15) is dimensionless. We set $M^2=1 \text{ GeV}^2$ [27].

The power-law behavior of the nFFs can be considered in different point of view: According to Eq. (15), at low value of β , the unintegrated gluon distribution $g(\beta, k_t^2; x_L)$ is defined as:

$$xg(\beta, Q^2; x_L) = \int_0^{Q^2} g(\beta, k_t^2; x_L) dk_t^2 \quad (20)$$

$g(\beta, k_t^2; x_L)$ satisfy the BFKL evolution equation:

$$\frac{dg(\beta, k_t^2; x_L)}{d \ln(1/x)} = K_L \otimes g = \lambda g \quad (21)$$

where \otimes stands for convolution and K_L is the Lipatov kernel which represent the sum over powers of $\alpha_s \ln(1/x)$ terms [21]. From Eq. (21) it is obvious that the function g follows a power-law behaviour in the variable β . Therefore, the gluon distribution can be expressed as:

$$xg(\beta, Q^2; x_L) \propto f(Q^2) \beta^{-\lambda} \quad (22)$$

The special case for which DGLAP equations can be solved analytically is the double leading log approximation (DLL) [19], which is based on the small x limit. The DLL solution represents as:

$$g(x, Q^2) = e^{2\sqrt{\alpha'_s \ln \frac{Q^2}{Q_0^2} \ln \frac{1}{x}}} g(x, Q_0^2) \quad (23)$$

here $\alpha'_s = \frac{3\alpha_s}{\pi}$ and $g(x, Q_0^2)$ is the gluon distribution at factorisation scale Q_0 [19].

In addition, The rise of $F_2(x, Q^2)$ at low x can be studied using the following structure function derivative [28]:

$$\lambda(x, Q^2) = -\left(\frac{\partial \ln F_2(x, Q^2)}{\partial \ln x}\right)_{Q^2} \quad (24)$$

According to the H1 publication [29], $\lambda(x, Q^2)$ does not depend on x , for $x \lesssim 0.01$. If we consider the fitting procedure of the form of $F_2(x, Q^2) = c(Q^2) \cdot x^{-\lambda(Q^2)}$ to the H1 structure function data [29], we see that in the region of $x \lesssim 0.01$, there is a nice agreement with the form of $\lambda(Q^2) = a \ln \frac{Q^2}{\Lambda^2}$ and H1 data. Now Let's come back to our input in Eq. (18). There are two terms in our proposed model, that they explain nFFs behavior at small value of β : $\beta^{-D_2^i+1}$ and $\beta^{-D_1^i \log(1 + \frac{Q_0^2}{q_0^2})}$. When ones compare the latter term with the above information, they would find out that Eq. (18) is not a weird form for gluon and sea quark densities. It is just like a window that gives us a new perspective on these distribution functions.

As mentioned in Ref. [20], the structure functions of proton is the subsequence of quark density which depend on x and Q_0^2 (in this paper $Q_0^2 = Q^2$). In this reference the Quark-Parton model is used to extract the proton structure function (which depend on x and Q^2) and the gluon density as an input is not considered. Since nFFs are conditional PDFs, we propose our fractal model by inspiring from Ref. [20]. As outlined earlier, nFFs obey the DGLAP evolution equations at a fixed value of x_L . Therefore, we set the value of $Q_0^2 = 1 \text{ GeV}^2$ in Eq. (18) to be able to compare the result of this analysis with the previous one (which are also in initial value of $Q_0^2 = 1 \text{ GeV}^2$) [47, 60]. Convolution of nFFs with the Wilson coefficients, C_i , gives the Leading neutron transverse structure functions [47, 60]:

$$F_k^{Ln(3)}(\beta, Q^2; x_L) = \sum_i \int_\beta^1 \frac{d\xi}{\xi} \mathcal{M}_{i/p}^n(\beta, \mu_F^2; x_L) \times C_{ki}\left(\frac{\beta}{\xi}, \frac{Q^2}{\mu_F^2}, \alpha_s(\mu_R^2)\right) + \mathcal{O}\left(\frac{1}{Q^2}\right). \quad (25)$$

Since there are a few experimental data related to the Leading neutron production, in this analysis we assume the symmetric light quark distributions: $\mathcal{M}_{u/p}^n = \mathcal{M}_{\bar{u}/p}^n = \mathcal{M}_{d/p}^n = \mathcal{M}_{\bar{d}/p}^n = \mathcal{M}_{s/p}^n = \mathcal{M}_{\bar{s}/p}^n$. So, at the initial scale of $Q_0^2 = 1 \text{ GeV}^2$, we have the singlet and gluon distributions as inputs. As fully describe in Ref. [60], $g(x_L)$ can be described by common parameters of $B^g = B^q \equiv B$, $C^g = C^q \equiv C$ and $D^g = D^q \equiv D$. Therefore the Eq. 19 can be rewritten as: $g(x_L) = N_i x_L^{A_i} (1 - x_L)^B (1 + C x_L^D)$. There are two parameters that control the normalization of inputs: N_i and D_0^i . We considered these parameters as only one free parameter and we name it as: $\Gamma_i = N_i e^{D_0^i}$. As a results, It turns out that the model contains 13 free parameters to be determined using

the experimental data (Γ_i , A_i , B , C , D , q_0 , D_1^i , D_2^i , and D_3). To perform the analysis, we used QCDNUM package [62] to not only solve the DGLAP evolution equations for the integrated nFFs in Eq. (18), but also we use it to extract the Leading neutron transverse structure functions, $F_2^{Ln(3)}(\beta, Q^2; x_L)$ up to NLO QCD approximation. We did our analysis in Variable Flavour Number Scheme (VFNS), which means that when the Q^2 value is equal to the pole mass of the heavy quarks, c, b and t ($m_c=1.4$ GeV, $m_b=4.5$ GeV and $m_t=175$ GeV), the number of flavours change from n_f to n_f+1 . In addition, we set the strong coupling constant on its recently updated average, $\alpha_s(M_z) = 0.1177$ [63].

B. Experimental data

The production of Leading neutrons in the semi-inclusive process $e^+p \rightarrow e^+nX$ are considered by the ZEUS [45] and H1 [42] collaborations at HERA. The H1 experiment measured $F_2^{LN(3)}$ in the phase space defined as $6 < Q^2 < 100$ GeV², $1.5 * 10^{-4} < x < 3 * 10^{-2}$, the longitudinal momentum fraction $0.32 < x_L < 0.95$ and neutron transverse momentum $p_T \leq 200$ MeV. In this interaction, the proton, and positron beam energies are $E_p=920$ GeV and $E_e=27.6$ GeV, respectively. Notice that the small value of the transverse momentum increases the relative contribution of pion exchange [64, 65] and the maximum transverse momentum, p_T^{max} , is set to 200 MeV [41, 42]. ZEUS data also cover the large range of kinematics of $7 < Q^2 < 1000$ GeV², $1.1 * 10^{-4} < x < 3.2 * 10^{-2}$ and $0.2 < x_L < 1$. In this process, positron and proton energies are $E_e=27.5$ GeV and $E_p=820$ GeV, respectively and the value of the neutron scattering angle, θ_n , is smaller than 0.8 mrad. The transverse momentum of the neutron is given by $p_T \sim x_L E_p \theta_n$. In this global analysis, only H1-2010 data are included in fitting procedure. Fig. (2) confirms the validity of the fractal model in the kinematic region of $x < 0.01$ and $Q^2 > 7$ GeV². Therefore, we have limited ourselves to the 189 data points of H1 collaboration, which are compatible with this kinematic region.

C. χ^2 minimization and nFFs Uncertainties

The optimum parameter values of the nFFs at the initial scale of $Q_0^2=1$ GeV², we used the χ^2 function:

$$\chi^2 = \sum_{i=1}^N \frac{(D_i - T_i)^2}{\sigma_i^2} \quad (26)$$

where i labels the number of data points used in our analysis, D_i is the data points and T_i is the theoretical prediction, which depends on the input nFFs parameters. σ_i^2 are the experimental

and statistical errors on data points, added in quadrature. In our analysis, the χ^2 function is optimized by the CERN program MINUIT [66]. In table I, we give the best fit values of nFFs parameters at initial scale of $Q_0^2=1 \text{ GeV}^2$. Those parameters marked by (*) are set as fixed values in the final analysis. In Sec. IV we will discuss these obtained parameters in more detail. In high-energy processes with initial state hadrons, PDFs and reliable knowledge of their uncertainties are needed. PDF uncertainties stem from two sources: a) Theoretical uncertainties which are the consequences of several assumptions made, such as the truncation of the DGLAP perturbation expansion [67] b) Experimental uncertainties which are due to the statistical and systematical errors of the experimental data used in the global fit [68]. Besides various techniques such as Lagrange Multiplier method [69] and Neural Network, the Hessian method is also a reliable method to calculate the experimental uncertainties of PDFs [6, 70]. We have used it to extract the nFF uncertainties. We refer the reader to Refs [6, 70] for technical detail. In our NLO QCD analysis, the covariance matrix elements for 9 free parameters are given in table II.

TABLE I: The best values, obtained for free parameters in Eq. (18) at the initial scale of $Q_0^2 = 1 \text{ GeV}^2$ using the H1 experimental data.

Parameters	$\beta M_{\frac{i=g}{F}}^n(\beta, Q_0^2, x_L)$	$\beta M_{\frac{i=g}{F}}^n(\beta, Q_0^2, x_L)$
Γ_i	0.14 ± 0.02	0.61 ± 0.04
A_i	0*	0*
B	1.75 ± 0.02	1.75 ± 0.02
C	26.3 ± 1.1	26.3 ± 1.1
D	6.67 ± 0.10	6.67 ± 0.10
q_0	0.32 ± 0.02	0.32 ± 0.02
D_1^i	0.033 ± 0.009	0*
D_2^i	1.015 ± 0.008	1*
D_3	-0.62 ± 0.02	-0.62 ± 0.02

IV. RESULTS AND DISCUSSION

Let us now give the details of the fractal analysis. The optimum values obtained in our analysis are summarized in Table I.

In our analysis, the data set does not include the small values of x_L , so we choose the zero value for A_q and A_g parameters. We also obtained a small value with a large error for D_1^g . Therefore, we set its value equal to zero. Now the significant parameter is D_2^g which controls the small-

TABLE II: The correlation matrix elements for the 9 free parameters at NLO fit

	Γ_q	Γ_g	B	C	D	q_0	D_1^q	D_2^q	D_3
Γ_q	1								
Γ_g	0.274	1							
B	0.070	0.003	1						
C	-0.060	0.026	0.795	1					
D	-0.022	0.024	0.254	0.534	1				
q_0	-0.503	-0.806	0.127	0.097	0.138	1			
D_1^q	0.497	0.152	-0.008	-0.055	-0.049	-0.271	1		
D_2^q	-0.206	0.063	-0.019	0.014	0.003	-0.041	0.145	1	
D_3	-0.340	-0.583	0.093	0.068	0.099	0.243	-0.012	-0.021	1

β behavior of gluon FFs. This parameter has so much effect on χ^2 , so we set its value equal to 1. In this analysis, we obtained the value of normalized χ^2 or the χ^2 per degree of freedom as $\frac{\chi^2}{n.d.f} = \frac{217.91}{180} = 1.21$ which is almost reasonable value. Our inputs in Eq (18) consist of 13 parameters. In final global analysis we decided to fix 3 parameters. In comparison with the previous analyses [47, 60], the dependence of input to the fixed parameters reduced (in Ref. [60], input describe by 11 parameters and 4 parameters are considered to be fixed and in Ref. [47] there is 16 parameters and 8 parameters are chosen to be fixed). The singlet and gluon densities, $\beta\mathcal{M}_{i/p}^n(x, Q_0^2; x_L)$, resulting from our QCD analysis are shown in Fig. (3) at the initial scale of $Q_0^2=1 \text{ GeV}^2$ and at two different values of $x_L=0.455$ and 0.725 . The shaded bands correspond to the estimated uncertainties of at $\Delta\chi^2=1$ and $\Delta\chi^2=10.41$ for confidence region of 68% (see appendix A for more detail).

As shown in Fig. (4), our results, based on the fractal model, for $\beta\mathcal{M}_{i/p}^n(x, Q_0^2; x_L)$ is compared with those of SKTJ17 and F. Ceccopieri Models [47, 60]. The fractal nFFs seem valid up to the vertical line is shown in the figures, which confirm the validity of this model at low values of β . It appears that the upward behavior of the singlet fractal densities at low values of β (or x) consistent with those we expected from the behavior of the usual PDFs at low x . Fig. (5) nicely shows the self-similarity behavior of the nFFs in the fixed value of x_L . The left panel represents the log-log plot of the nFFs for singlet and gluon densities as a function of x for different values of Q^2 . The same log-log plot as a function of Q^2 for different values of x is shown in the right panel too. In Fig. (6), we present the comparison of our theoretical predictions for Leading neutron transverse structure functions, $F_2^{Ln}(\beta, x_L, Q^2)$, with H1-2010 experimental data [42]. In general, there is agreement between our analysis based on the fractal approach with these experimental data in

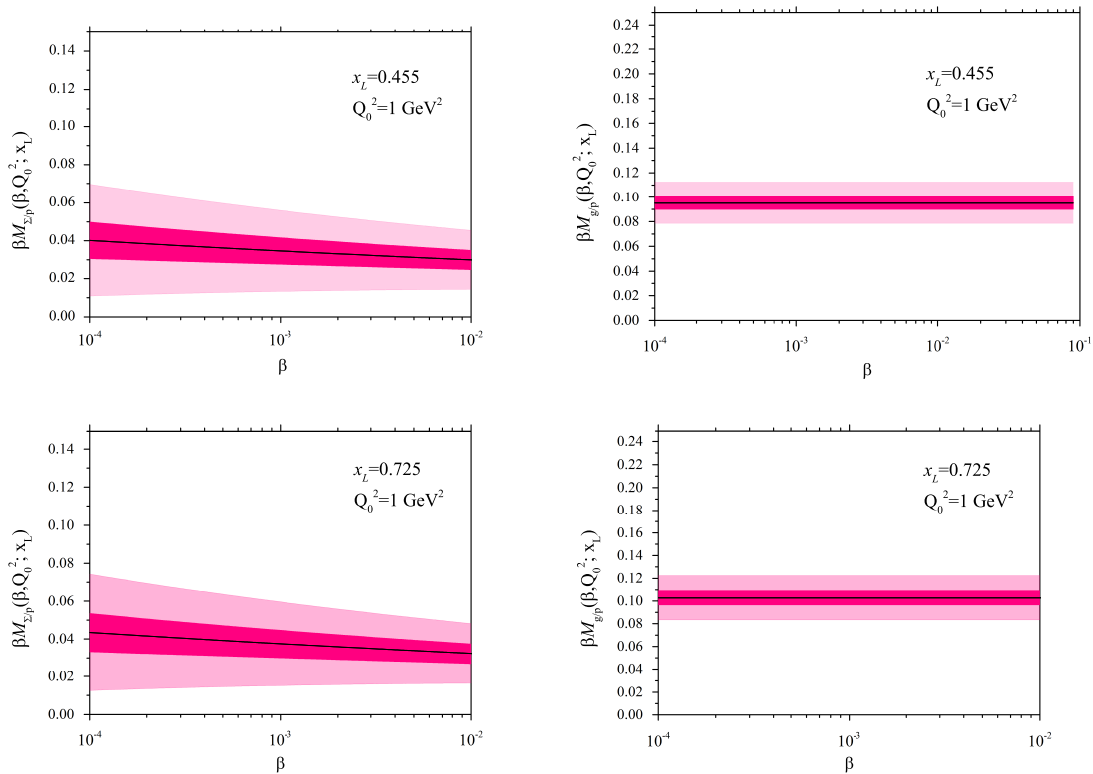


FIG. 3: (Color online). The singlet and gluon FFs as a function of β at the initial scale of $Q_0^2=1 \text{ GeV}^2$ for two different values of $x_L=0.455, 0.725$.

different values of β , Q^2 and x_L . Comparison between our result with those from experimental data and SKTJ17 model are shown in Fig. (7). The shaded bands of both models correspond to the estimated uncertainties of $\Delta\chi^2=1$. It seems that the uncertainties in the fractal approach reduce about 50%.

Finally, as a result of this analysis, we show that the nFFs can be described with a fractal or self-similar model at the low values of the fractional momentum β . Recently, we used the fractal approach to explore the behavior of un-polarized fragmentation functions (FFs) of the pion in the regions of small momentum fractions z [71]. We believe that it is possible to use the fractal framework to explore the low x behavior of the PDFs too. Work along this line is in progress. In summary, we show that the upward behavior of the nFFs for $x < 0.001$ and $Q^2 > 7\text{GeV}^2$ may be described by the self-similar behavior of these conditional PDFs. Such behavior has not been obtained in the last studies.

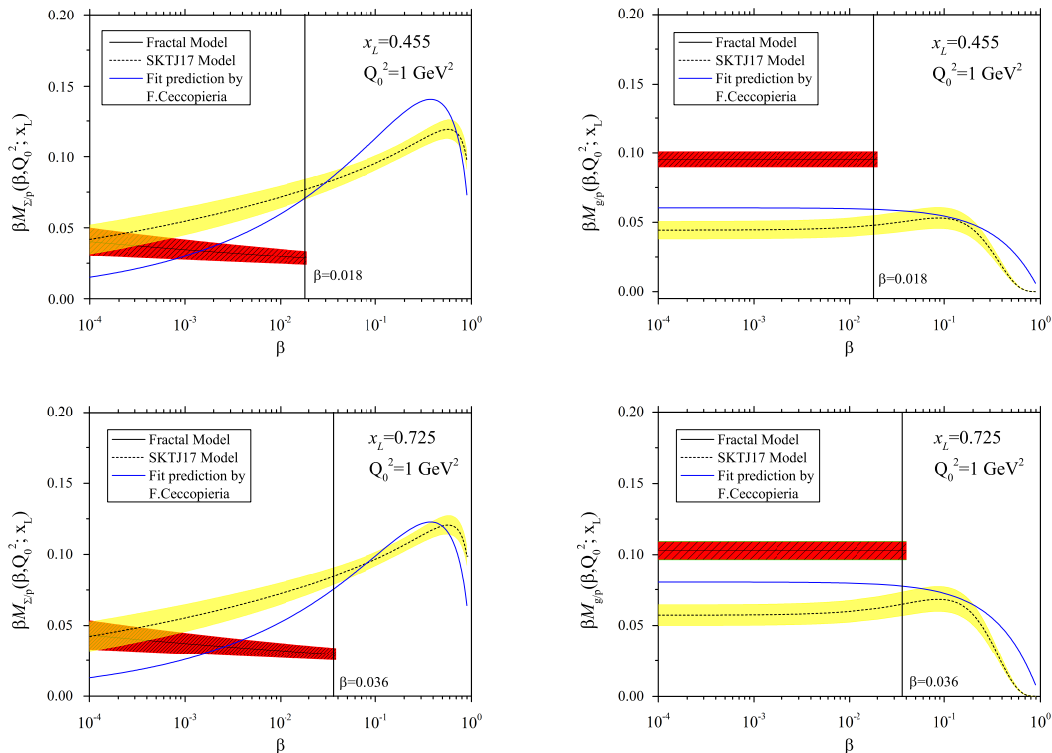


FIG. 4: (Color online) Comparing the singlet and gluon momentum distribution resulting from the fractal model with SKTJ17 model [47] and prediction proposed by F.Ceccopieri [60]

V. SUMMARY AND CONCLUSIONS

Fractals provide a different way to observe and model complex phenomena. Their applications in strong interaction open detail of high energy collisions such as ep scattering. In 2010 and the years before, several experiments are dedicated to the positron-proton collider at HERA in order to collect precision data for events with the final state related to the Leading neutron production. In this paper, we present the NLO QCD analysis of neutron FFs based on the fractal approach. We have performed an analysis using the H1-2010 Leading neutron production data. As a result, we have shown that the parameterized forms of the neutron FFs based on the fractal concept can give an appropriate description of the Leading neutron production mechanism. We used the Hessian method in order to explain the uncertainties of the nFFs and the corresponding observables.

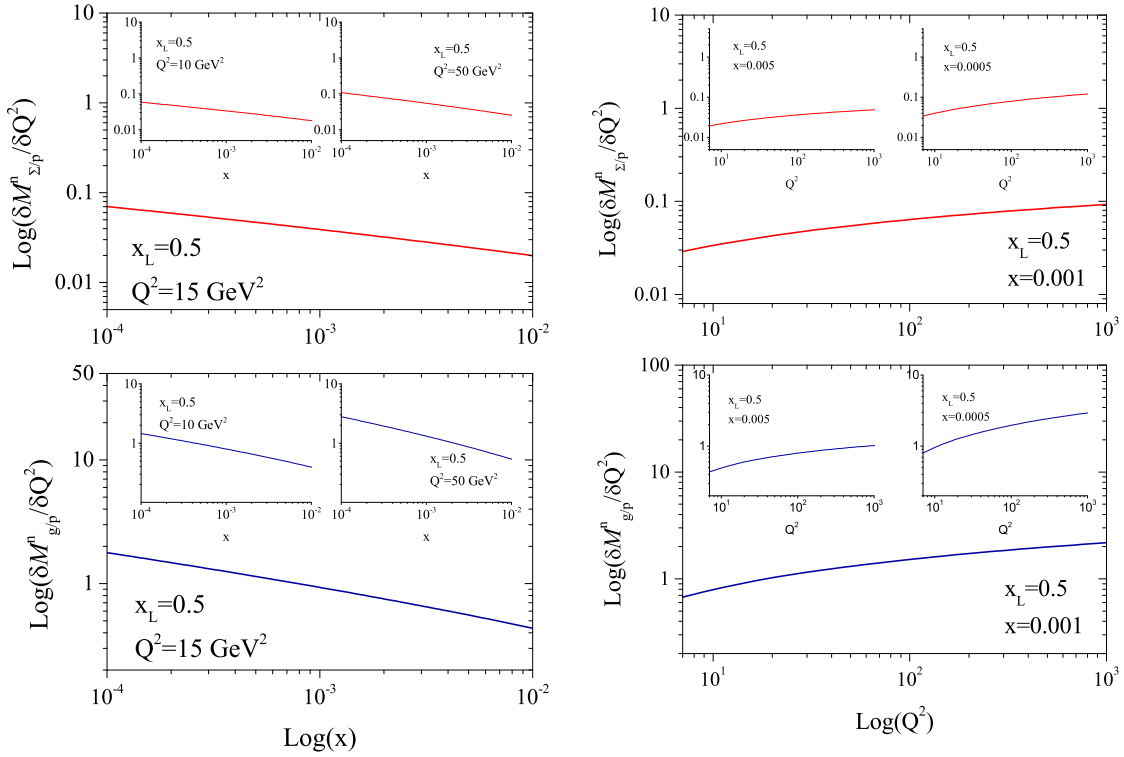


FIG. 5: (Color online) The self-similarity behavior of nFFs in the fixed value of $x_L=0.5$ for different values of x in some fixed values of Q^2 (left panel) and also in different values of Q^2 for some fixed values of x (right panel).

Acknowledgements

We gratefully acknowledge to Professor Firooz Arash for carefully reading the manuscript, many helpful discussions, and comments. F. Taghavi Shahri also is thankful to Ferdowsi University of Mashhad for the financial support provided for this research. This work is supported by the Ferdowsi University of Mashhad under grant number 73209(25/12/1397).

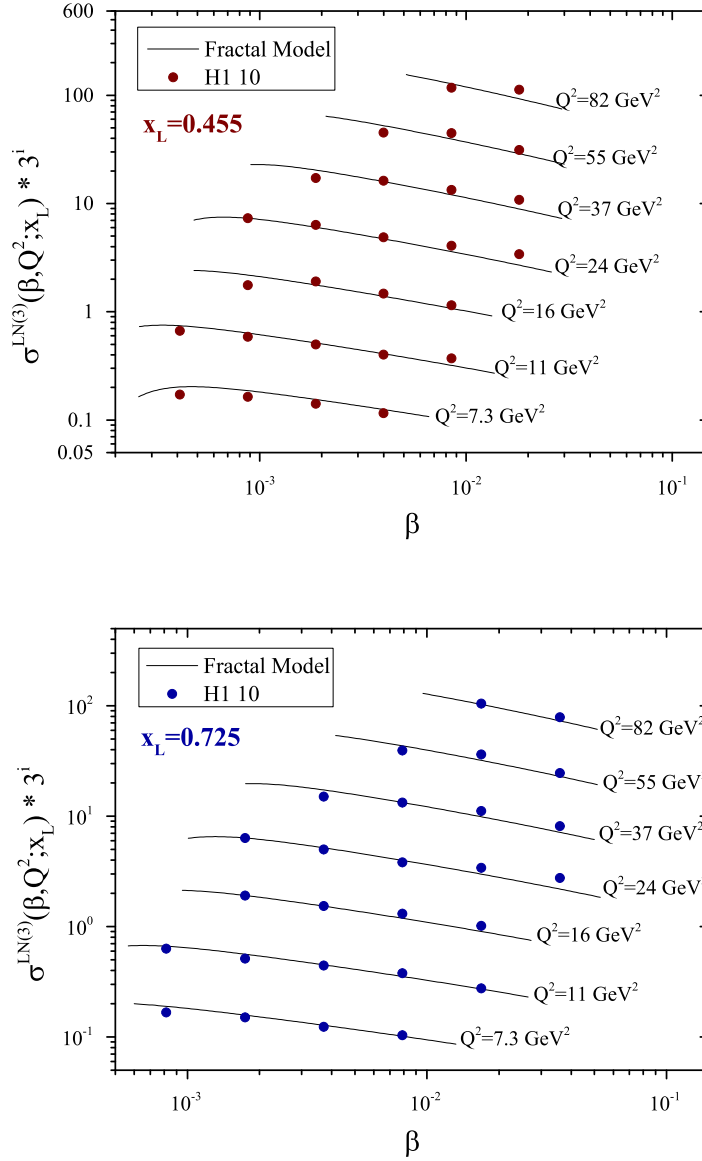


FIG. 6: (Color online) The comparison of H1-2010 experimental data with Leading neutron transverse structure function, $F_2(\beta, Q^2; x_L)$, as a function of β for some selected values of Q^2 at fixed values of $x_L = 0.455, 0.725$. To facilitate the graphical presentation, we have plotted $F_2(\beta, Q^2; x_L) * 3^i$.

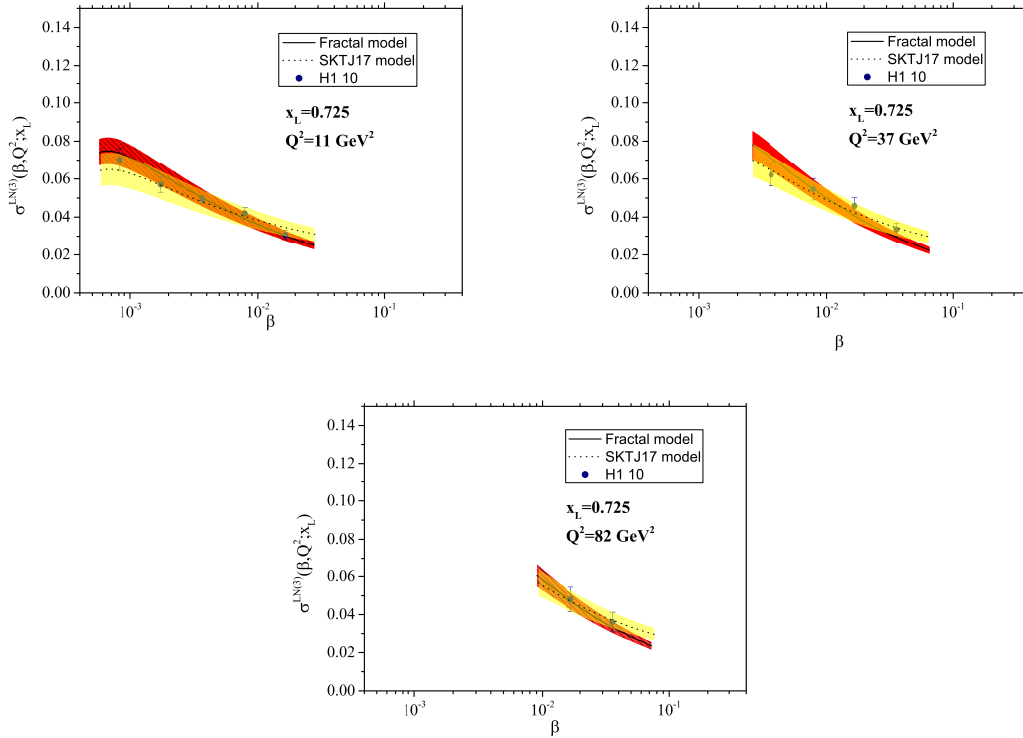


FIG. 7: (Color online) The comparison of H1-2010 experimental data with the experimental observables resulting from the fractal model and SKTJ17 model [47], as a function of β for some selected values of $Q^2=11, 37, 82 \text{ GeV}^2$ at fixed value of $x_L = 0.725$.

Appendices

Appendix A

The experimental uncertainties of fractal nFFs are estimated by a general statistical method named as Hessian method. If the optimized parameters of each distribution obtained in this analysis present by p_i^0 ($i=1,2,3, \dots, N$), the quadratic expansion of the χ^2 around the minimum point p^0 is written as:

$$\Delta\chi^2 = \chi^2(p^0 + \delta p) - \chi^2(p^0) = \sum_{i,j} H_{ij} \delta p_i \delta p_j$$

In this Taylor series expansion, the first derivative terms vanish at the minimum point and H_{ij} is the Hessian matrix defined as

$$H_{ij} = \frac{1}{2} \frac{\partial^2 \chi^2}{\partial p_i \partial p_j} \Big|_{min}$$

The uncertainty on a quantity $F(x, p^0)$ is then calculated by linear error propagation:

$$\Delta F = \left[\Delta \chi_{\text{global}}^2 \sum_{i,j=1}^k \frac{\partial F}{\partial p_i} H_{ij}^{-1} \frac{\partial F}{\partial p_j} \right]^{\frac{1}{2}} .$$

in order to determine the nFFs uncertainties, the confidence region of χ^2 distribution should be estimated. This region can be identified by an ellipsoid on this normal distribution and it is defined by $\Delta \chi^2$. The confidence level P for the χ^2 distribution with N degrees of freedom is written as:

$$P = \int_0^{\Delta \chi^2} \frac{(\chi^2)^{\frac{N}{2}-1}}{2^{\frac{N}{2}} \Gamma(\frac{N}{2})} e^{-\frac{\chi^2}{2}} d\chi^2 = P(\approx 0.68) ,$$

In this analysis, we consider the one- σ -error range, therefore the confidence level value is $P = 0.68$. Since there are 9 free parameters in the final fitting procedure, by using the above equation, we obtain the value of $\Delta \chi^2 = 10.41$.

-
- [1] C. Bourrely, Phys. Rev. C **98**, no. 5, 055202 (2018) doi:10.1103/PhysRevC.98.055202 [arXiv:1810.08445 [hep-ph]].
- [2] R. Abdul Khalek *et al.*, arXiv:1905.04311 [hep-ph].
- [3] F. Zaidi, H. Haider, M. Sajjad Athar, S. K. Singh and I. Ruiz Simo, arXiv:1903.09000 [hep-ph].
- [4] L. A. Harland-Lang, A. D. Martin, P. Motylinski and R. S. Thorne, “Parton distributions in the LHC era: MMHT 2014 PDFs,” Eur. Phys. J. C **75**, no. 5, 204 (2015) doi:10.1140/epjc/s10052-015-3397-6 [arXiv:1412.3989 [hep-ph]].
- [5] R. D. Ball *et al.* [NNPDF Collaboration], “Parton distributions for the LHC Run II,” JHEP **1504**, 040 (2015) doi:10.1007/JHEP04(2015)040 [arXiv:1410.8849 [hep-ph]].
- [6] A. D. Martin, W. J. Stirling, R. S. Thorne and G. Watt, “Parton distributions for the LHC,” Eur. Phys. J. C **63**, 189 (2009) doi:10.1140/epjc/s10052-009-1072-5 [arXiv:0901.0002 [hep-ph]].
- [7] S. Alekhin, J. Blümlein and S. Moch, Eur. Phys. J. C **78**, no. 6, 477 (2018) doi:10.1140/epjc/s10052-018-5947-1 [arXiv:1803.07537 [hep-ph]].
- [8] M. Salajegheh, M. Nejad, A. Mirjalili and S. Atashbar Tehrani, arXiv:1904.03439 [hep-ph].
- [9] I. Abt, A. M. Cooper-Sarkar, B. Foster, V. Myronenko, K. Wichmann and M. Wing, Phys. Rev. D **94**, no. 3, 034032 (2016) doi:10.1103/PhysRevD.94.034032 [arXiv:1604.02299 [hep-ph]].
- [10] H. Abdolmaleki *et al.* [xFitter Developers’ Team], Eur. Phys. J. C **78**, no. 8, 621 (2018) doi:10.1140/epjc/s10052-018-6090-8 [arXiv:1802.00064 [hep-ph]].
- [11] S. Heidari, B. Rezaei, J. K. Sarma and G. R. Boroun, Nucl. Phys. A **986**, 195 (2019). doi:10.1016/j.nuclphysa.2019.03.005
- [12] I. M. Dremin, Mod. Phys. Lett. A **3**, 1333 (1988). doi:10.1142/S0217732388001604
- [13] P. Lipa and B. Buschbeck, Phys. Lett. B **223**, 465 (1989). doi:10.1016/0370-2693(89)91634-1
- [14] W. Florkowski and R. C. Hwa, Phys. Rev. D **43**, 1548 (1991). doi:10.1103/PhysRevD.43.1548
- [15] J. D. Bjorken, In *Eilat 1994, Proceedings, Deep inelastic scattering and related subjects* 151-176, and SLAC Stanford - SLAC-PUB-6477 (94/04,rec.Jul.) 33 p
- [16] A. Bhattacharya, B. Chakrabarti, T. Sarkhel and S. N. Banerjee, Int. J. Mod. Phys. A **15**, 2053 (2000). doi:10.1016/S0217-751X(00)00083-5
- [17] B. B. Mandelbrot, The Fractal Geometry of Nature., W. H. Freeman, New York 1977.
- [18] I. M. Dremin and B. B. Levchenko, Phys. Lett. B **292**, 155 (1992). doi:10.1016/0370-2693(92)90623-C
- [19] M. Ninomiya and K. Watanabe, Nuovo Cim. A **37**, 343 (1977) doi:10.1007/BF02909267
- [20] T. Lastovicka, Eur. Phys. J. C **24**, 529 (2002) doi:10.1007/s10052-002-8893-9 [hep-ph/0203260].
- [21] T. Lastovicka, doi:10.3204/DESY-THESIS-2004-016
- [22] D. K. Choudhury and R. Gogoi, hep-ph/0310260.
- [23] D. K. Choudhury and R. Gogoi, hep-ph/0503047.
- [24] A. Jahan and D. K. Choudhury, arXiv:1106.1145 [hep-ph].

- [25] D. K. Choudhury and A. Jahan, *Int. J. Mod. Phys. A* **28**, 1350079 (2013) doi:10.1142/S0217751X13500796 [arXiv:1305.6180 [hep-ph]].
- [26] A. Jahan and D. K. Choudhury, *J. Phys. Conf. Ser.* **481**, 012025 (2014). doi:10.1088/1742-6596/481/1/012025
- [27] A. Jahan and D. K. Choudhury, *Phys. Rev. D* **89**, no. 1, 014014 (2014) doi:10.1103/PhysRevD.89.014014 [arXiv:1401.4327 [hep-ph]].
- [28] C. Adloff *et al.* [H1], *Phys. Lett. B* **520**, 183-190 (2001) doi:10.1016/S0370-2693(01)01074-7 [arXiv:hep-ex/0108035 [hep-ex]].
- [29] C. Adloff *et al.* [H1], *Eur. Phys. J. C* **21**, 33-61 (2001) doi:10.1007/s100520100720 [arXiv:hep-ex/0012053 [hep-ex]].
- [30] D. K. Choudhury, B. Saikia and K. Kalita, *Int. J. Mod. Phys. A* **32**, no. 18, 1750107 (2017) doi:10.1142/S0217751X1750107X [arXiv:1608.02771 [hep-ph]].
- [31] A. Deppman and E. Megias, *EPJ Web Conf.* **141**, 01011 (2017) doi:10.1051/epjconf/201714101011 [arXiv:1610.09928 [hep-ph]].
- [32] D. de Florian, M. Epele, R. J. Hernandez-Pinto, R. Sassot and M. Stratmann, *Phys. Rev. D* **95**, no. 9, 094019 (2017) doi:10.1103/PhysRevD.95.094019 [arXiv:1702.06353 [hep-ph]].
- [33] V. Bertone *et al.* [NNPDF Collaboration], *Eur. Phys. J. C* **77**, no. 8, 516 (2017) doi:10.1140/epjc/s10052-017-5088-y [arXiv:1706.07049 [hep-ph]].
- [34] D. P. Anderle, F. Ringer and M. Stratmann, *Phys. Rev. D* **92**, no. 11, 114017 (2015) doi:10.1103/PhysRevD.92.114017 [arXiv:1510.05845 [hep-ph]].
- [35] J. J. Ethier, N. Sato and W. Melnitchouk, *Phys. Rev. Lett.* **119**, no. 13, 132001 (2017) doi:10.1103/PhysRevLett.119.132001 [arXiv:1705.05889 [hep-ph]].
- [36] G. Altarelli, R. K. Ellis, G. Martinelli and S. Y. Pi, *Nucl. Phys. B* **160**, 301 (1979). doi:10.1016/0550-3213(79)90062-2
- [37] D. de Florian and R. Sassot, *Phys. Rev. D* **56**, 426 (1997) doi:10.1103/PhysRevD.56.426 [hep-ph/9703228].
- [38] A. Daleo and R. Sassot, *Nucl. Phys. B* **673**, 357 (2003) doi:10.1016/j.nuclphysb.2003.09.007 [hep-ph/0309073].
- [39] L. Trentadue and G. Veneziano, *Phys. Lett. B* **323**, 201 (1994). doi:10.1016/0370-2693(94)90292-5
- [40] L. Trentadue, *Nucl. Phys. Proc. Suppl.* **39BC**, 50 (1995) doi:10.1016/0920-5632(95)00043-9 [hep-ph/9506324].
- [41] C. Adloff *et al.* [H1 Collaboration], *Eur. Phys. J. C* **6**, 587 (1999) doi:10.1007/s100529901072 [hep-ex/9811013].
- [42] F. D. Aaron *et al.* [H1 Collaboration], *Eur. Phys. J. C* **68**, 381 (2010) doi:10.1140/epjc/s10052-010-1369-4 [arXiv:1001.0532 [hep-ex]].
- [43] S. Chekanov *et al.* [ZEUS Collaboration], *JHEP* **0906**, 074 (2009) doi:10.1088/1126-6708/2009/06/074 [arXiv:0812.2416 [hep-ex]].

- [44] S. Chekanov *et al.* [ZEUS Collaboration], Nucl. Phys. B **658**, 3 (2003) doi:10.1016/S0550-3213(03)00152-4 [hep-ex/0210029].
- [45] S. Chekanov *et al.* [ZEUS Collaboration], Nucl. Phys. B **637**, 3 (2002) doi:10.1016/S0550-3213(02)00439-X [hep-ex/0205076].
- [46] L. Rinaldi, doi:10.3204/DESY-THESIS-2006-028
- [47] S. Shoeibi, H. Khanpour, F. Taghavi-Shahri and K. Javidan, Phys. Rev. D **95**, no. 7, 074011 (2017) doi:10.1103/PhysRevD.95.074011 [arXiv:1703.04369 [hep-ph]].
- [48] C. Adloff *et al.* [H1], Eur. Phys. J. C **6**, 587-602 (1999) doi:10.1007/s100529901072 [arXiv:hep-ex/9811013 [hep-ex]].
- [49] D. de Florian and R. Sassot, Phys. Rev. D **58**, 054003 (1998) doi:10.1103/PhysRevD.58.054003 [hep-ph/9804240].
- [50] F. A. Ceccopieri and L. Trentadue, Phys. Lett. B **655**, 15 (2007) doi:10.1016/j.physletb.2007.07.074 [arXiv:0705.2326 [hep-ph]].
- [51] G. Altarelli and G. Parisi, Nucl. Phys. B **126**, 298 (1977). doi:10.1016/0550-3213(77)90384-4
- [52] J. A. M. Vermaseren, A. Vogt and S. Moch, Nucl. Phys. B **724**, 3 (2005) doi:10.1016/j.nuclphysb.2005.06.020 [hep-ph/0504242].
- [53] J. Benecke, T. T. Chou, C. N. Yang and E. Yen, Phys. Rev. **188**, 2159 (1969). doi:10.1103/PhysRev.188.2159
- [54] T. T. Chou and C. N. Yang, Phys. Rev. D **50**, 590 (1994). doi:10.1103/PhysRevD.50.590
- [55] F. Arash, Phys. Lett. B **557**, 38 (2003) doi:10.1016/S0370-2693(03)00177-1 [hep-ph/0301260].
- [56] J. R. McKenney, N. Sato, W. Melnitchouk and C. R. Ji, Phys. Rev. D **93**, no. 5, 054011 (2016) doi:10.1103/PhysRevD.93.054011 [arXiv:1512.04459 [hep-ph]].
- [57] P. C. Barry, N. Sato, W. Melnitchouk and C. R. Ji, arXiv:1804.01965 [hep-ph].
- [58] J. Pumplin, D. Stump, R. Brock, D. Casey, J. Huston, J. Kalk, H. L. Lai and W. K. Tung, Phys. Rev. D **65**, 014013 (2001) doi:10.1103/PhysRevD.65.014013 [hep-ph/0101032].
- [59] S. Shoeibi, F. Taghavi-Shahri, H. Khanpour and K. Javidan, Phys. Rev. D **97**, no. 7, 074013 (2018) doi:10.1103/PhysRevD.97.074013 [arXiv:1710.06329 [hep-ph]].
- [60] F. A. Ceccopieri, Eur. Phys. J. C **74**, no. 8, 3029 (2014) doi:10.1140/epjc/s10052-014-3029-6 [arXiv:1406.0754 [hep-ph]].
- [61] K. K. Sharma, A. C. Katoch and R. C. Verma, Z. Phys. C **75**, 253 (1997) doi:10.1007/s002880050468 [hep-ph/9507358].
- [62] M. Botje, Comput. Phys. Commun. **182**, 490 (2011) doi:10.1016/j.cpc.2010.10.020 [arXiv:1005.1481 [hep-ph]].
- [63] D. d'Enterria *et al.*, arXiv:1512.05194 [hep-ph].
- [64] H. Holtmann, G. Levman, N. N. Nikolaev, A. Szczurek and J. Speth, Phys. Lett. B **338**, 363 (1994). doi:10.1016/0370-2693(94)91392-7
- [65] B. Kopeliovich, B. Povh and I. Potashnikova, Z. Phys. C **73**, 125 (1996) doi:10.1007/s002880050301

- [hep-ph/9601291].
- [66] F. James, CERN-D-506, CERN-D506.
- [67] A. D. Martin, R. G. Roberts, W. J. Stirling and R. S. Thorne, *Eur. Phys. J. C* **35**, 325 (2004) doi:10.1140/epjc/s2004-01825-2 [hep-ph/0308087].
- [68] A. D. Martin, R. G. Roberts, W. J. Stirling and R. S. Thorne, *Eur. Phys. J. C* **28**, 455 (2003) doi:10.1140/epjc/s2003-01196-2 [hep-ph/0211080].
- [69] D. Stump, J. Pumplin, R. Brock, D. Casey, J. Huston, J. Kalk, H. L. Lai and W. K. Tung, *Phys. Rev. D* **65**, 014012 (2001) doi:10.1103/PhysRevD.65.014012 [hep-ph/0101051].
- [70] J. Pumplin, D. Stump, R. Brock, D. Casey, J. Huston, J. Kalk, H. L. Lai and W. K. Tung, *Phys. Rev. D* **65**, 014013 (2001) doi:10.1103/PhysRevD.65.014013 [hep-ph/0101032].
- [71] A. Mohamaditabar, F. Taghavi-Shahri and S. Shoeibi, *Eur. Phys. J. A* **56**, no.3, 77 (2020) doi:10.1140/epja/s10050-020-00087-y